Research Article

Effects of Hall current and permeability on the stability of peristaltic flow

Kh. S. Mekheimer[1] · B. M. Shankar[2] · R. E. Abo-Elkhair[1]

Received: 31 August 2019 / Accepted: 7 November 2019 / Published online: 14 November 2019

Abstract
Pumping molecules and atoms near or along surfaces under the perturbing influence of surface acoustic wave is important in micro-flow systems. These micro-flow systems can circulate heat-transfer fluids over silicon chips, reconstitute dried drugs and possibly synthesize chemicals from liquid to solid constituents. The stability of acoustic streaming flow induced by a small-amplitude surface acoustic wave propagating along the walls of a confined parallel-plane channel with a magneto incompressible fluid through a porous medium is considered. The stability related to the flow initiated by the peristaltic waves propagating along the deformable walls is explored numerically. The neutral stability boundary is gotten by understanding the significant Orr–Sommerfeld condition. The Chebyshev collocation method is employed to solve the resulting generalized eigenvalue problem. The critical Reynolds number and the corresponding wave number are obtained for different values of $K_0 = c/u_{max}$ (ratio of the wave speed to the maximum speed of the basic flow), magnetic field M, Hall current β_1 and permeability parameter k. Different values of the critical Reynolds number are obtained when $K_0 = c/u_{max}$=1 (rigid wall) and ≠ 1for deformable walls. It is found that the critical Reynolds number (when the wall is deformable; $K_0 = 10$) becomes 577.22 which is much less than conventional rigid-wall case [5772, obtained by Orszag using the spectral method (Orszag in J Fluid Mech 50:689–703. https://doi.org/10.1017/S0022112071002842, 1971)]. The effect of incrementing of K_0 and k shows destabilizing effect on the fluid flow while increasing in the values of M and β_1 exhibits a stabilizing influence on the fluid flow. So, various kinds of noises like Hall current, permeability and peristaltic waves propagating along the walls will premature any instability mechanism considering the temporal growth of the disturbances. Also, the range of wave numbers relevant to the peristaltic wave or the Reynolds number of this basic flow must be carefully selected for the optimal flow control usage in bio-MEMS.

Keywords Peristaltic transport · Stability analysis · Hall currents · MHD · Porous medium

1 Introduction

Surface acoustic wave (SAW) is an interesting and important subject in physics as well as in many other scientific applications. Microchannels built in MEMS (MicroElectro-Mechanical System) are easily subjected to environment noises, such as oscillations or vibrations, externally excited traveling waves (SAW). The last one is normally related to the peristaltic transport as the wall is flexible. Recent progress in MEMS technology supplies micro-fluid system manufacture and application multiplicity. Because the micro-fluid systems have the advantages of minuscule size and are facile to carry, they additionally have high precision and short replication time. Experimental and theoretical results [1, 2] show that the flow velocity is proportional to the second power of the SAW displacement velocity

✉ Kh. S. Mekheimer, kh_mekheimer@azhar.edu.eg; B. M. Shankar, bmshankar@pes.edu; R. E. Abo-Elkhair, elkhair33@yahoo.com | [1]Department of Mathematics, Faculty of Science, Al-Azhar University, Nasr City, Cairo 11884, Egypt. [2]Department of Mathematics, PES University, Bangalore 560 085, India.

in these microchannels. Additionally, transport phenomena by surface acoustic wave SAW are consequential in pumping molecules and atoms near or along surfaces under the perturbing influence. In fact, with the latter, it has been reported that people can make micro-flow systems that could circulate heat-transfer fluids over silicon chips, reconstitute dried drugs and possibly synthesize chemicals from liquid to solid constituents [3]. Moreover, peristalsis is well known to physiologists to be one of the major mechanisms for fluid transport in many biological systems. In particular, peristaltic mechanism may be involved in urine transport from kidney to bladder through the ureter, movement of chyme in the gastrointestinal tract, transport of spermatozoa in the ductus efferentes of the male reproductive tracts, and in the cervical canal and in the flow of blood [4–10]. In addition, peristaltic pumping occurs in many practical applications involving biomechanical systems [11–13].

The Orr–Sommerfeld equation governs the linear stability characteristics of a basic two-dimensional incompressible laminar parallel flow with respect to an infinitesimal disturbance. The difficulties associated with solving this eigenvalue problem are well known. No exact solution of this equation has been obtained for a general velocity profile, except for a constant plane Poiseuille flow. Numerous methods have been presented to calculate the eigenvalues and eigenfunctions of the Orr–Sommerfeld (O–S) equation [14]. O–S equation has been applied for investigating the stability of channel flow, Blasius boundary layer profile, shear layer, laminar jet and developed wake. The stability characteristic for the acoustic streaming flow is thus of considerable importance to the flow control or mixing in micro-domain since the bulk (cross-sectional) size of the microchannel is at most a few tens of $O(m)$ and the wall of the microchannel is almost in submicrons or lesser. As we know, it is necessary to obtain curves of the neutral stability boundary from the stability equation (Orr–Sommerfeld equation) and associated boundary conditions for the description of the hydrodynamical transition to turbulence in normal fluids. The stability characteristics thus obtained is crucial to the flow control and understanding of the flow transition in bio-MEMS or even in nanobiotechnology systems. Only a few [15, 16] investigated the stability problem linked to those basic flows (induced by the peristaltic transport) where, the flexible wall or the wall deformation effect is represented by the phase speed of the peristaltic wave, c and by using the verified numerical code (Spectral method) [17, 18]. They found that the critical Reynolds number Re_c for a deformable wall is less than that for a rigid-wall case ($\backsim$ 5772, obtained by Orszag using the spectral method [19]). In this work, we shall investigate the stability quandary linked to a magneto-fluid with Hall current through a porous medium (induced by the peristaltic motion) utilizing the verified numerical code (via the spectral method [17]). The paper is organized as follows: we shall first derive the basic equations and boundary conditions in Sect. 2. Perturbed systems presented in Sect. 3. Section 4 states the primary flow stability and modified Orr–Sommerfeld equation. Numerical solution and the validation of our results considered in Sects. 5 and 6. Curves of the neutral stability boundary from the stability equation is provided and discussed in Sect. 7. Conclusion and the main finding are in Sect. 8. The prefatory results display that both the effects of the permeability and peristaltic transport ($\frac{c}{u_{\max}} > 1$)will degrade the flow stability significantly.

2 Basic equations and formulation of the problem

Consider a two-dimensional infinite channel of uniform thickness $2h$, and filled with an incompressible, viscous and electrically conducting fluid. We introduce Cartesian coordinate system with the x-axis along the center line of the channel and y-axis normal to it. A constant magnetic field $B = (0, 0, B_o)$ is applied on the flow. The walls of the channel are wavy on which imposed traveling sinusoidal waves of small amplitude. We neglect the induced magnetic field under the assumption that the magnetic Reynolds number is small.

The equations of motion and continuity governing this model together with generalized Ohm's law taking Hall effect are [5]:

$$\rho\left[\frac{\partial \underline{V}}{\partial t} + (\underline{V}\cdot\underline{\nabla})\underline{V}\right] = -\underline{\nabla}p + \underline{\nabla}\cdot\underline{S} + \underline{J}\times\underline{B} + \underline{R}, \tag{1}$$

$$\underline{\nabla}\cdot\underline{V} = 0, \tag{2}$$

$$\underline{J} = \sigma\left[\underline{E} + \underline{V}\times\underline{B}\right] - \frac{\sigma}{en_e}\underline{J}\times\underline{B}, \tag{3}$$

$$\underline{\nabla}\times\underline{H} = \underline{J}, \qquad \underline{\nabla}\times\underline{E} = 0, \qquad \underline{\nabla}\cdot\underline{B} = 0. \tag{4}$$

where $\rho, t, \nu, p, \mu, \sigma, e$, and n^e are the density of fluid, time, kinematic viscosity, pressure, dynamic viscosity, electrical conductivity, electric charge and number density of electrons, respectively. V, J, B, E and H are the velocity vector, electric current density, magnetic induction vector, intensity of the electric field and magnetic field strength, respectively.

From Eq. (4) for the current density $J = (J_x, J_y, J_z)$, we obtain from the relation $\underline{\nabla}\cdot\underline{J} = 0$, that J_z = constant.

Hence, we consider that the channel is non-conducting and therefore $J_z = 0$ at the channel.

The constitutive equation for stress tensor $\underline{S}$ is

$$\underline{S} = \mu\left[(\text{grad}\,\underline{V}) + (\text{grad}\,\underline{V})^{\mathrm{T}}\right].$$

The Darcy's resistance has been written as

$$\underline{R} = -\frac{\mu}{k}\underline{V}.$$

Here, k (positive value) is the permeability of the porous medium. In the absence of an externally applied electric field and with negligible effects of polarization of the ionized gas, we assume that the electric field vector equals zero, i.e., $\underline{E} = 0$. The x- and y-components of Eq. (1) are:

$$\rho\left[\frac{\partial u}{\partial t} + u\frac{\partial u}{\partial x} + v\frac{\partial u}{\partial y}\right] = -\frac{\partial p}{\partial x} + \frac{\partial S_{xx}}{\partial x} + \frac{\partial S_{xy}}{\partial y} - \frac{\sigma B_0^2}{\left(1+m_1^2\right)}\left(u - m_1 v\right) + R_x, \tag{5}$$

$$\rho\left[\frac{\partial v}{\partial t} + u\frac{\partial v}{\partial x} + v\frac{\partial v}{\partial y}\right] = -\frac{\partial p}{\partial y} + \frac{\partial S_{yx}}{\partial x} + \frac{\partial S_{yy}}{\partial y} - \frac{\sigma B_0^2}{\left(1+m_1^2\right)}\left(v + m_1 v\right) + R_y, \tag{6}$$

where R_x and R_y are the x- and y-components of R and S_{xx}, S_{xy} and S_{yy} are to be computed from the constitutive equation of the stress tensor, u and v are the velocity components in the direction of increasing x and y, respectively, and $m_1 = \left(\frac{\sigma B_0}{en_e}\right)$ is the Hall parameter.

From Eqs. (2), (5) and (6), we obtain:

$$\left[\frac{\partial u}{\partial t} + u\frac{\partial u}{\partial x} + v\frac{\partial u}{\partial y}\right] = -\frac{1}{\rho}\frac{\partial p}{\partial x} + \nu\nabla^2 u - \frac{sB_0^2}{\rho\left(1+m_1^2\right)}\left(u - m_1 v\right) - \frac{\nu}{k}u, \tag{7}$$

$$\left[\frac{\partial v}{\partial t} + u\frac{\partial v}{\partial x} + v\frac{\partial v}{\partial y}\right] = -\frac{1}{\rho}\frac{\partial p}{\partial y} + \nu\nabla^2 v - \frac{sB_0^2}{\rho\left(1+m_1^2\right)}\left(v + m_1 v\right) - \frac{\nu}{k}v. \tag{8}$$

The fluid is subjected to boundary conditions imposed by the symmetric motion of the flexible walls. Let the vertical displacements of the upper and lower walls be η and $-\eta$ respectively, $\eta(x,t) = a\cos\left(\frac{2\pi}{\lambda}(x - ct)\right)$, where a is the amplitude, λ is the wave length, and c is the wave speed. The horizontal displacement will be assumed zero (Fig. 1).

The boundary conditions are

$$u(x, \pm h \pm \eta, t) = 0, \tag{9}$$

$$v(x, \pm h \pm \eta, t) = \pm\frac{\partial \eta(x,t)}{\partial t}. \tag{10}$$

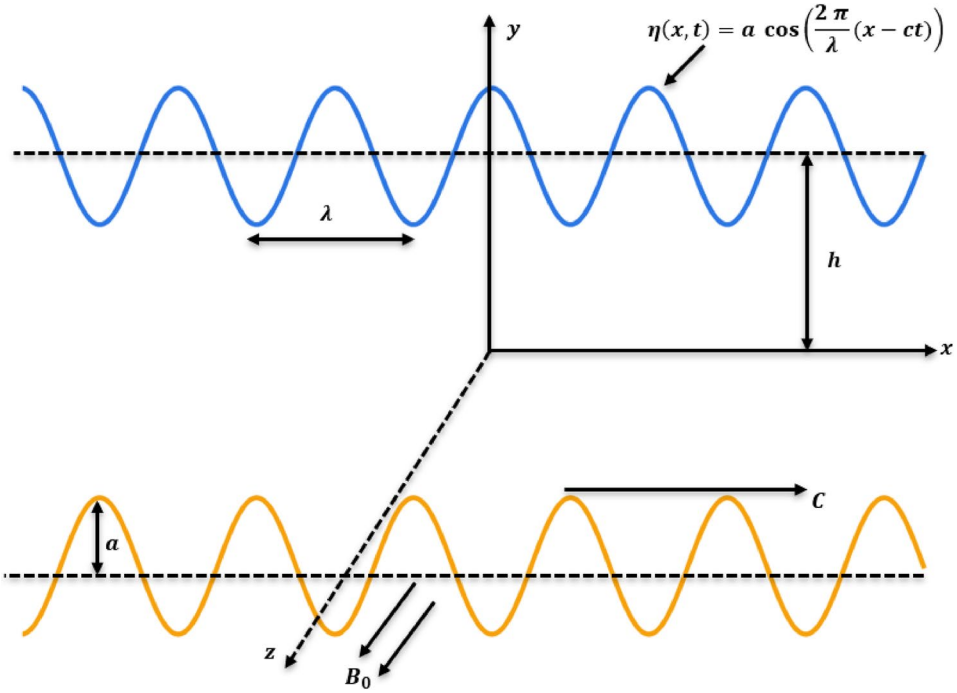

Fig. 1 Geometry of the problem

Equation (2) allows the use of the stream function $\psi(x, y, t)$ in terms of which

$$u = \frac{\partial \psi}{\partial y}, \quad v = -\frac{\partial \psi}{\partial x}. \tag{11}$$

Introducing the dimensionless variables

$$x^* = \frac{x}{h}, y^* = \frac{y}{h}, u^* = \frac{u}{c}, v^* = \frac{v}{c}, \psi^* = \frac{\psi}{ch}, \eta^* = \frac{\eta}{h},$$
$$= t^* \frac{ct}{h}, {m_1}^* = \frac{m_1}{\rho h}, \; p^* = \frac{p}{\rho c^2}, \frac{1}{k^*} = \frac{\nu h}{kc}.$$

After dropping the asterisks and eliminating the pressure p from Eqs. (7) and (8), we obtain

$$\left[\frac{\partial}{\partial t}\left(\nabla^2 \psi\right) + \psi_y \nabla^2 \psi_x - \psi_x \nabla^2 \psi_y\right] + M^2 \beta_1 \nabla^2 \psi$$
$$+ \frac{1}{k}\nabla^2 \psi = \frac{1}{\mathrm{Re}_{sw}} \nabla^4 \psi, \qquad \eta(x, t) = \varepsilon \cos\, a\,(x - t), \tag{12}$$

with boundary conditions

$$\psi_y = 0, \psi_x = \mp\, \alpha\varepsilon \sin \alpha\,(x - t) \quad \text{at}$$
$$y = \pm\, 1 \pm \eta(x, t), \tag{13}$$

where $\varepsilon = \frac{a}{h}$ is the amplitude ratio, $\alpha = \frac{2\pi h}{\lambda}$ is the wave number, $\mathrm{Re}_{sw} = \frac{ch}{\nu}$ is the Reynolds number, $M = \sqrt{\frac{h\sigma}{\rho c}} B_0$ is the Hartman number and $\beta_1 = \frac{1}{1 + m_1^2}$ is the Hall current parameter.

3 Perturbed systems

Assuming the amplitude ratio ε of the wave to be small, we obtain the solution for the stream function as a power series in terms of ε by expanding ψ and $\frac{\partial p}{\partial x}$ in the form [2]:

$$\psi = \psi_0 + \varepsilon\psi_1 + \varepsilon^2 \psi_2 + \cdots, \tag{14}$$

$$\left(\frac{\partial p}{\partial x}\right) = \left(\frac{\partial p}{\partial x}\right)_0 + \varepsilon\left(\frac{\partial p}{\partial x}\right)_1 + \varepsilon^2\left(\frac{\partial p}{\partial x}\right)_2 + \cdots. \tag{15}$$

The first term at the right-hand side corresponds to an imposed pressure gradient which is considered as a constant. The higher-order terms correspond to the peristaltic motion. Collecting the terms of like powers of ε, we obtain three sets of coupled linear differential equations with their corresponding boundary conditions.

System of Order Zero

$$\frac{1}{\mathrm{Re}_{sw}} \nabla^2 \nabla^2 \psi_0 = \left(\frac{\partial}{\partial t}\nabla^2 \psi_0 + \psi_{0y} \nabla^2 \psi_{0x} - \psi_{0x} \nabla^2 \psi_{0y} + \right)$$
$$+ \left(M^2 \beta_1 + \frac{1}{k}\right) \nabla^2 \psi_0, \tag{16}$$

$$\psi_{0y}(\pm\, 1) = 0,$$
$$\psi_{0x}(\pm\, 1) = 0. \tag{17}$$

System of Order One

$$\frac{1}{\mathrm{Re}_{sw}} \nabla^2 \nabla^2 \psi_1 = \left(\frac{\partial}{\partial t}\nabla^2 \psi_1 + \psi_{0y} \nabla^2 \psi_{1x} + \psi_{1y} \nabla^2 \psi_{0x}\right.$$
$$\left. - \psi_{0x} \nabla^2 \psi_{1y} - \psi_{1x} \nabla^2 \psi_{0y}\right) + \left(M^2 \beta_1 + \frac{1}{k}\right) \nabla^2 \psi_1, \tag{18}$$

$$\psi_{1y}(\pm 1) \pm \psi_{0yy}(\pm 1) \cos a(x - t) = 0,$$
$$\psi_{1y}(\pm 1) \pm \psi_{1xy}(\pm 1) \cos a(x - t) = \mp a \sin\,(x - t). \tag{19}$$

We note that the first set of differential equations in ψ_0 subject to the steady parallel flow and transverse symmetry assumption for a constant pressure gradient in the x -direction yields the following flow:

$$\psi_0(y) = \frac{K_0}{\Gamma^2}\left[y - \frac{\sinh \Gamma\, y}{\Gamma \cos h \Gamma}\right], \tag{20}$$

where $K_0 = \frac{\mathrm{Re}_{sw}}{2}\left(-\frac{\partial p}{\partial x}\right)_0$, the necessary pumping to sustain a plane Poiseuille flow (pressure-driven case) [2], and $\Gamma^2 = (M^2 \beta_1 + \frac{1}{k})$.

The differential equations in ψ_1 with their corresponding boundary conditions are satisfied by

$$\psi_1(x, y, t) = \frac{1}{2}\left(\phi_1(y) e^{i\alpha(x-t)} + \phi_1^*(y) e^{-i\alpha(x-t)}\right), \tag{21}$$

where the asterisk denotes the complex conjugate. Substituting with Eqs. (21) in (18) yields the first-order equation for a magneto-fluid through a porous medium:

$$i\alpha \mathrm{Re}_{sw}\left[\left(\overline{u} - 1\right)\left(D^2 - \alpha^2\right) - D^2 \overline{u}\right] \phi_1$$
$$+ \left(M^2 \beta_1 + \frac{1}{k}\right)(D^2 - \alpha^2)\phi_1(y) = \left(D^2 - \alpha^2\right)^2 \phi_1(y), \tag{22}$$

where $D = \frac{\mathrm{d}}{\mathrm{d}y}$. The normal fluid is subjected to boundary conditions imposed by the symmetric motion of the wavy walls. The basic flow now has the form, as $\overline{u} = \frac{\partial \psi_0}{\partial y}$:

$$\overline{u} = \frac{K_0}{\Gamma^2}\left[1 - \frac{\cosh(\Gamma y)}{\cosh(\Gamma)}\right]. \tag{23}$$

Table 1 Process of convergence of the Chebyshev collocation method for different values of physical parameters

N	$M=0.01,\beta_1=0.05,k=1,K_0=1$		$M=1,\beta_1=0.05,k=1,K_0=1$		$M=0.01,\beta_1=2,k=1,K_0=1$		$M=0.01,\beta_1=0.05,k=10,K_0=1$		$M=0.01,\beta_1=0.05,k=1,K_0=10$	
	Re_c	α_c	Re_c	α_c	Re_c	α_c	Re_c	α_c	Re_c	α_c
10	21516.4585	0.9615	21916.9145	0.9674	21518.0434	0.9615	4880.4651	1.0776	2151.6458	0.9615
15	14660.4704	0.9652	15259.5226	0.9635	14662.798	0.9652	6347.7567	1.0163	1466.047	0.9652
20	14256.9094	0.9715	14826.8214	0.9697	14259.1033	0.9715	6392.987	1.0143	1425.6909	0.9715
25	14253.8806	0.9716	14822.7849	0.9698	14256.0707	0.9716	6392.8389	1.0143	1425.388	0.9716
30	14253.8905	0.9716	14822.7939	0.9698	14256.0805	0.9716	6392.839	1.0143	1425.389	0.9716
35	14253.8905	0.9716	14822.7939	0.9698	14256.0805	0.9716	6392.839	1.0143	1425.389	0.9716

Table 2 Comparison of results between published and the present work when $M, \beta_1 \to 0$ and $k \to \infty$

K_0	Chu [16]	Present work	
	Re_c	Re_c	α_c
1	5772	5772.2218	1.0205
2	2886.5	2886.1109	1.0205
10	577.25	577.2221	1.0205

If we take $\Gamma \to 0$, i.e, $M \to 0$, $\beta_1 \to 0, k \to \infty \Rightarrow \overline{u}) = \frac{K_0}{2}(1-y^2)$,

$$\phi_1(\pm 1) = \pm 1, \quad \phi_{1y}(\pm 1) = \frac{k_0}{\Gamma}\tanh(\Gamma).$$

4 Primary flow stability and modified Orr–Sommerfeld (O–S) equation

To obtain the stability characteristics for acoustic streaming flows by using verified codes developed before [15, 16] (calculating the Orr–Sommerfeld spectra), we need to transform Eq. 22 into the modified Orr–Sommerfeld (Orr–Sommerfeld for a magneto-fluid with permeability) form by resealing and redimensionalization of physical parameters and variables mentioned before (e.g., the careful selection of K_0 and c). Thus, we have the linearized disturbance equation

$$i\alpha Re\left[(\overline{u}-C)\left(D^2-\alpha^2\right)-D^2\overline{u}\right]\phi_1 + \left(M^2\beta_1+\frac{1}{k}\right)(D^2-\alpha^2)\phi_1(y) = \left(D^2-\alpha^2\right)^2\phi_1(y), \tag{24}$$

where $Re = \frac{u_{\max}h}{\nu}$ is the Reynolds number, $C = C_r + iC_i$, where C is the ratio between the velocity of the propagating perturbation wave and the characteristic velocity, and C_i is the amplification factor. As for the temporal stability problem, in which the growth or decay of a disturbance in time is considered, we treat the complex wave speed C as the eigenvalue parameter of the problem.

The fluid is subjected to boundary conditions imposed by the symmetric motion of the walls and the no-slip condition at walls. The basic flow now has this form [19, 20] or comparing the definition of Re and Rec above, the mean (basic) velocity profile is then given by

$$\overline{u} = \frac{c}{u_{\max}\Gamma^2}\left[1-\frac{\cosh\Gamma y}{\cosh\Gamma}\right], \tag{25}$$

where $K_0 = \frac{c}{u_{\max}}$ and c is the phase speed of the peristaltic wave. This basic flow comes from the fluid-wall interaction

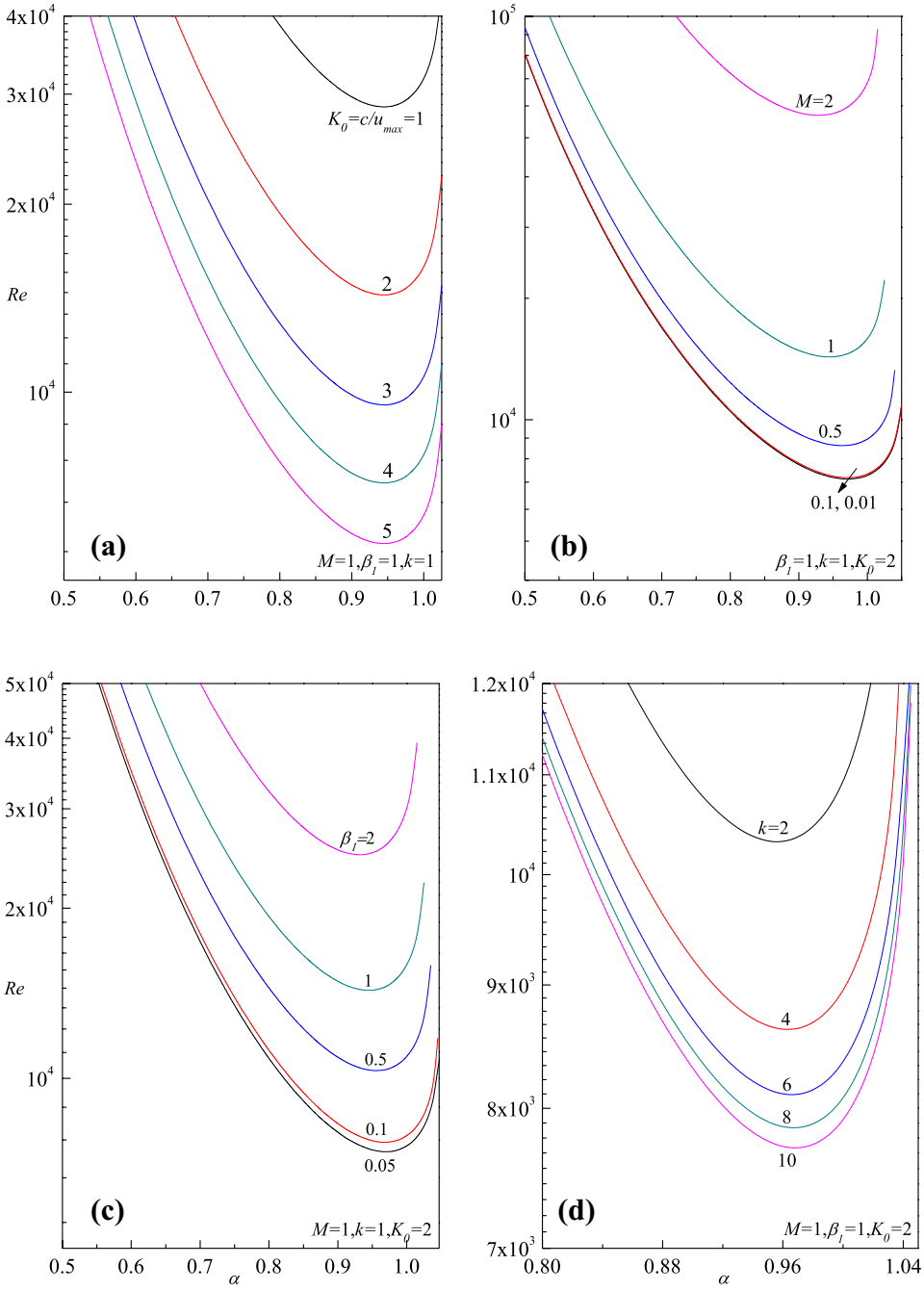

Fig. 2 Neutral stability curves for different values of **a** $K_0(= c/u_{max})$ **b** Hartman number M **c** Hall current β_1 **d** permeability k

(the small-amplitude peristaltic waves propagating along the walls), and boundary conditions remain the same as that in [15, 16] as we only have interests in the stability boundary for the primary flow induced by the peristaltic transport [15, 16]. The flexible wall effect is represented by the phase speed of the peristaltic wave, c. The effect of the wall deformation, being of the order of magnitude (ϵ^2) [18], is rather small (say, ϵ 0.01) and will not be considered here. The boundary conditions for ϕ or D ϕ are already defined in the form

$$\phi_1(\pm 1) = \pm 1, \quad \phi_{1y}(\pm 1) = \frac{K_0}{\Gamma}\tanh(\Gamma). \tag{26}$$

In the limit as $M \to 0$ and $k \to \infty$ we obtained the same results for the Orr–Sommerfeld equation and boundary conditions as in [16].

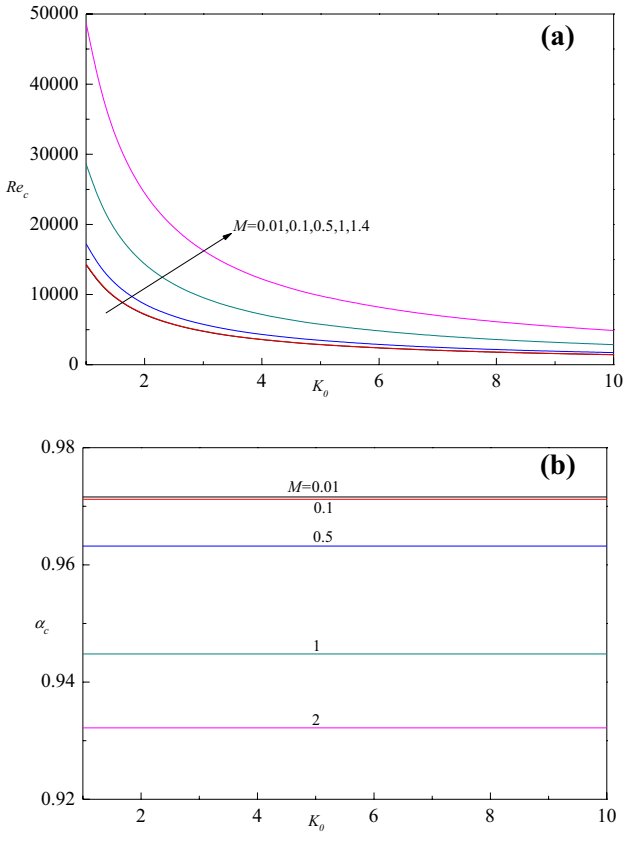

Fig. 3 Variation of M on **a** critical Reynolds number Re_c **b** critical wave number α_c as a function of K_0 for $\beta_1 = 1$and $k = 1$

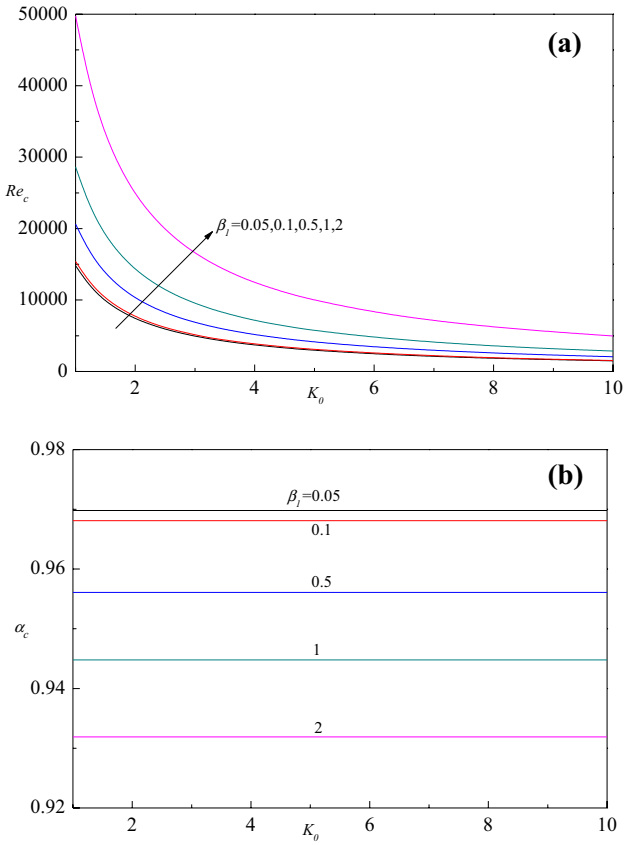

Fig. 4 Variation of β_1 on **a** critical Reynolds number Re_c **b** critical wave number α_c as a function of K_0 for $M = 1$and $K = 1$

5 Numerical solution

In Chebyshev collocation method, first we expand ϕ_1 in the form

$$\phi_{1n}(y) = \sum_{n=0}^{N} \left(1 - y^2\right)^2 T_{2n-2}(y), \tag{27}$$

where $\phi_{1n}(y)$ satisfies the boundary conditions as in [1] and $T_n(y)$ is the Chebyshev polynomial defined by

$$\begin{aligned} T_{n+1}(y) - 2yT_n(y) + T_{n-1}(y) = 0, \qquad & T_0(y) = 1, \\ T_1(y) = y, \qquad & (-1 \le y \le 1). \end{aligned} \tag{28}$$

Using Eq. (27) into Eq. (28) and requiring that Eq. (28) be satisfied at Ncollocation points $y_1, y_2, \ldots, y_N$, where

$$y_m = \cos\left(\frac{m-1}{2N-1}p\right) (m = 1, 2, \ldots, N), \tag{29}$$

we obtain Nalgebraic equations for Nunknowns $a_1, a_2, \ldots, a_N$.

$$AX = CBX, \tag{30}$$

where $X^{\mathrm{T}} = (a_1, a_2, \ldots, a_N)$ is the transpose of the column vector X. The coefficient matrices A and B are of dimensions $N \times N$ and are defined as

$$\begin{aligned} A = {} & \bar{u}(y_m)\left(D^2 - \alpha^2\right)\phi_{1n}(y_m) - D^2\bar{u}(y_m)\phi_{1n}(y_m) \\ & - \frac{1}{i\alpha\mathrm{Re}}\left[\left(D^2 - \alpha^2\right)^2\phi_{1n}(y_m)\right] \\ & - \left(M^2\beta_1 + \frac{1}{k}\right)\left[\left(D^2 - \alpha^2\right)\phi_{1n}(y_m)\right], \end{aligned} \tag{31}$$

$$B = \left(D^2 - \alpha^2\right)_{1n}(y_m). \tag{32}$$

For the constant values of all the dimensionless parameters concerned therein, the eigenvalue ensure compose definite a non-trivial solution of Eq. (30) is achieved. From $N + 1$ eigenvalues, $C(1), C(2), \cdots, C(N + 1)$ the one having the largest imaginary part of ($C(p)$, say) is selected. To obtain the neutral stability curve, the value of Re where the imaginary part of $C(p)$ disappears is sought. Let this value of Re be Re_T . The lowest point of Re_T as a function of α gives the critical Reynolds number Re_c and the critical wave number α_c . The real part of $C(p)$ corresponding to Re_c and α_c gives the critical wave speed C_c (Shankar and

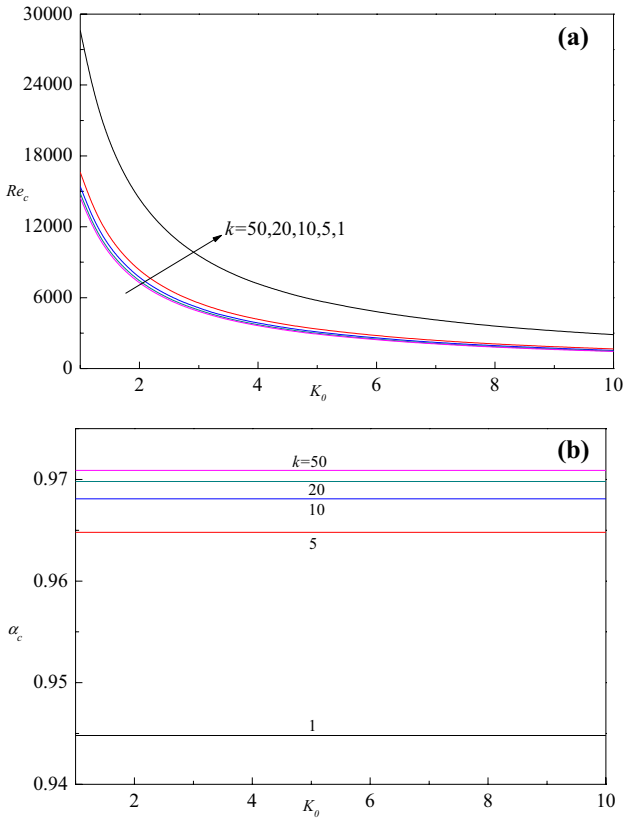

Fig. 5 Variation of k on **a** critical Reynolds number Re_c **b** critical wave number α_c as a function of K_0 for $M = 1$and $\beta_1 = 1$

Shivakumara [21]). This procedure is repeated for different values of governing parameters involved therein. A suitable environment for the implementation of these steps is carried out using the software program Mathematica 11.3 (© Wolfram Research).

6 Convergence and validation of results

First, the Chebyshev collocation method convergence is examined by increasing in the Chebyshev polynomial, which is shown in Table 1. It is observed that the results continue steady and the accurateness is improved up to 4 digits for $N = 35$ and noted that increasing any physical parameters considered do not affect the convergence process and hence the results are obtained by taking $N = 35$. Verification of the computer code is established by comparing our data with published results. The critical stability parameters computed for different values of K_0 under the limiting case of $M, \beta_1 \to 0, k \to \infty$ are compared with those of [16] in Table 2 and it is seen that the agreement is good. The above two tests present a strong confirmation of our numerical code/results.

7 Results and discussion

The typical neutral stability curves in the (α, Re) -plane represent the threshold between stable and unstable modes are shown in Fig. 2 for various values of K_0 (Fig. 2a), M (Fig. 2b),β_1 (Fig. 2c) and k (Fig. 2d). The region over and under each neutral stability curve corresponds to the unstable and stability region, respectively. The stability region, identifiable to the minimum of the Reynolds number, gets decreased with increasing K_0 and k, that is, the instability region is pushed downward. This behavior is reversed with increasing M and β_1 values.

The computed values of critical stability parameters $(\alpha_c, \mathrm{Re}_c)$ as a function of K_0 for several values of physical parameters are shown in Figs. 3, 4 and 5. As observed in Figs. 3a, 4a and 5a, the value of critical Reynolds number is monotonically decreasing functions of K_0 and finally tends to a steady value as K_0 turns out to be large for all values of physical parameters considered. The dependence of α_c upon K_0 is constant irrespective of all the values of physical parameters (Figs. 3b, 4b and 5b).

Figure 3a displays the trend of Re_c versus K_0 for various values of M ranging from 0.01 to 2 when $\beta_1 = 1, k = 1$. The curves of $M = 0.01$has the lowest value of Re_c. The increase in the values of M leads to more stable in the system. Figure 3b shows that the size of the convection cell becomes larger as M increases.

Figure 4a, b distinctly illustrates variation of $(\mathrm{Re}_c, \alpha_c)$ as a function of K_0 for several values of β_1. Figure 4a signified that increasing β_1 exhibits stabilizing effect on the system. Increasing $\beta_1$diminishes critical values of wave number suggesting its outcome is to enhance the cell width size (Fig. 4b).

Figure 5a, b displays the variation of $(\mathrm{Re}_c, \alpha_c)$ and K_0 for different values of k. The onset of convection is advanced with an increase in the value of k. The cell width decreases with increasing k (Fig. 5b).

8 Conclusions

The effect of Hall current on the stability of peristaltic transport of a magneto-fluid in a horizontal Darcy porous channel is investigated numerically by employing Chebyshev collocation method (generalized eigenvalue problem). The effect of increasing K_0 and k is decreasing the stability region while increasing the value of M and β_1 exhibits a stabilizing influence on the fluid flow. Also, it is noticed that the critical values of Reynolds number turn out to be invariant as K_0 becomes large; however, wave number is independent of K_0. Cell width size increases with an increase in M and β_1, whereas the opposite effect

is seen with the increase in *k*. Finally , we can conclude that various kinds of MEMS-environmental noises will premature any instability mechanism considering the temporal growth of the disturbances. Either the range of wave numbers is relevant to the peristaltic wave or the Reynolds number of the basic MHD flows with permeability must be carefully selected for MEMS-applications, like the optimal flow control, drag reduction of micro air vehicles (MAV), DNA manipulations in ambient fluids and micro-flow mixing or osmosis.

Compliance with ethical standards

Conflict interest The author declare that they have no conflict interest.

References

1. Chu KHW (2001) Transport within a microtube induced by a surface acoustic wave. EPJ Appl Phys 13:147–152. https://doi.org/10.1051/epjap:2001126
2. Chu K-HW (2002) Peristaltic transport within a micro-tube. Phys Scr 65:283–288. https://doi.org/10.1238/physica.regular.065a00283
3. Moroney RM, White RM, Howe RT (1991) Microtransport induced by ultrasonic Lamb waves. Appl Phys Lett 59:774–776. https://doi.org/10.1063/1.105339
4. Abdelsalam SI, Bhatti MM (2019) New insight into AuNP applications in tumour treatment and cosmetics through wavy annuli at the nanoscale. Sci Rep 9:260. https://doi.org/10.1038/s41598-018-36459-0
5. Abdelsalam SI, Bhatti MM (2018) The study of non-Newtonian nanofluid with hall and ion slip effects on peristaltically induced motion in a non-uniform channel. RSC Adv 8:7904–7915. https://doi.org/10.1039/c7ra13188g
6. Abdelsalam SI, Vafai K (2017) Combined effects of magnetic field and rheological properties on the peristaltic flow of a compressible fluid in a microfluidic channel. Eur J Mech B Fluids 65:398–411. https://doi.org/10.1016/j.euromechflu.2017.02.002
7. Abd elmaboud Y, Abdelsalam SI, Mekheimer KhS (2018) Couple stress fluid flow in a rotating channel with peristalsis. J Hydrodyn 30:307–316. https://doi.org/10.1007/s42241-018-0037-2
8. Mekheimer KhS, Komy SR, Abdelsalam SI (2013) Simultaneous effects of magnetic field and space porosity on compressible Maxwell fluid transport induced by a surface acoustic wave in a microchannel. Chin Phys B. https://doi.org/10.1088/1674-1056/22/12/124702
9. Ellahi R, Zeeshan A, Hussain F, Asadollahi A (2019) Peristaltic blood flow of couple stress fluid suspended with nanoparticles under the influence of chemical reaction and activation energy. Symmetry (Basel) 11:276. https://doi.org/10.3390/sym11020276
10. Bhatti MM, Zeeshan A, Ellahi R, Shit GC (2018) Mathematical modeling of heat and mass transfer effects on MHD peristaltic propulsion of two-phase flow through a Darcy–Brinkman–Forchheimer porous medium. Adv Powder Technol 29:1189–1197. https://doi.org/10.1016/j.apt.2018.02.010
11. Bhatti MM, Zeeshan A, Ellahi R, Ijaz N (2017) Heat and mass transfer of two-phase flow with Electric double layer effects induced due to peristaltic propulsion in the presence of transverse magnetic field. J Mol Liq 230:237–246. https://doi.org/10.1016/j.molliq.2017.01.033
12. Ellahi R, Raza M, Akbar NS (2017) Study of peristaltic flow of nanofluid with entropy generation in a porous medium. J Porous Media 20:461–478. https://doi.org/10.1615/JPorMedia.v20.i5.70
13. Abo-Elkhair RE, Mekheimer KhS, Moawad AMA (2019) Combine impacts of electrokinetic variable viscosity and partial slip on peristaltic MHD flow through a micro-channel. Iran J Sci Technol Trans A Sci 43:201–212. https://doi.org/10.1007/s40995-017-0374-y
14. Lam TT, Bayazitoglu Y (1986) Solution to the Orr–Sommerfeld equation for liquid film flowing down an inclined plane: an optimal approach. Int J Numer Methods Fluids 6:883–894. https://doi.org/10.1002/fld.1650061203
15. Chu AKH (2003) Stability of slip flows in a peristaltic transport. Europhys Lett 64:435–440. https://doi.org/10.1209/epl/i2003-00220-2
16. Chu ZK-H (2003) Stability of flows in a peristaltic transport. Mech Res Commun 30:623–628. https://doi.org/10.1016/S0093-6413(03)00065-X
17. Chu WKH (2001) Spectra of the Orr–Sommerfeld equation: the plane Poiseuille flow for the normal fluid revisited. J Phys A Math Gen 34:3389–3392. https://doi.org/10.1088/0305-4470/34/16/306
18. Orszag SA (1971) Accurate solution of the Orr–Sommerfeld stability equation. J Fluid Mech 50:689–703. https://doi.org/10.1017/S0022112071002842
19. Fung YC, Yih CS (1964) Peristaltic transport. J Appl Mech Trans ASME 35:669–675. https://doi.org/10.1115/1.3601290
20. Chu WKH, Fang J (2000) On the peristaltic transport in Small–Knudsen–Number flow. Meccanica 35:69–74. https://doi.org/10.1023/A:1004804829239
21. Shankar BM, Shivakumara IS (2018) Stability of penetrative natural convection in a non-Newtonian fluid-saturated vertical porous layer. Transp Porous Media 124:395–411. https://doi.org/10.1007/s11242-018-1074-6